Published in final edited form as:
Neuroimage. 2012 February 1; 59(3): 2529–2538. doi:10.1016/j.neuroimage.2011.08.094.

Bedside optical imaging of occipital resting-state functional connectivity in neonates

Brian R. White[a,1], **Steve M. Liao**[b,1], **Silvina L. Ferradal**[c], **Terrie E. Inder**[b,d,e], and **Joseph P. Culver**[a,c,d,*]

[a]Department of Physics, Washington University, One Brookings Drive, St. Louis, MO 63130, USA

[b]Department of Pediatrics, Washington University School of Medicine, 660 S. Euclid Ave., St. Louis, MO 63110, USA

[c]Department of Biomedical Engineering, Washington University, One Brookings Drive, Washington University, St. Louis, MO 63130, USA

[d]Department of Radiology, Washington University School of Medicine, 660 S. Euclid Ave., St. Louis, MO 63110, USA

[e]Department of Neurology, Washington University School of Medicine, 660 S. Euclid Ave., St. Louis, MO 63110, USA

Abstract

Resting-state networks derived from temporal correlations of spontaneous hemodynamic fluctuations have been extensively used to elucidate the functional organization of the brain in adults and infants. We have previously developed functional connectivity diffuse optical tomography methods in adults, and we now apply these techniques to study functional connectivity in newborn infants at the bedside. We present functional connectivity maps in the occipital cortices obtained from healthy term-born infants and premature infants, including one infant with an occipital stroke. Our results suggest that functional connectivity diffuse optical tomography has potential as a valuable clinical tool for the early detection of functional deficits and for providing prognostic information on future development.

Keywords

Resting state; Functional connectivity; Neonates; Prematurity; Optical tomography

Introduction

Survival rates for preterm infants have improved dramatically in recent decades due to advances in perinatal and neonatal care. However, this reduction in mortality has not translated into a reduction in neurodevelopmental morbidity (Fanaroff et al., 2003). More than one half of preterm infants will suffer from neurobehavioral (or functional) impairments in a broad range of motor, cognitive, and behavioral domains (Holsti et al., 2002; Taylor et al., 2004; Woodward et al., 2009), placing a significant burden on families

*Corresponding author at: Washington University School of Medicine, Department of Radiology, 4525 Scott Avenue, Room 1137, Saint Louis, MO, 63110, USA. Fax: +1 314 747 5191. culverj@mir.wustl.edu (J.P. Culver)..
whiteb@wusm.wustl.edu (B.R. White), liao_s@kids.wustl.edu (S.M. Liao), sferrada@wustl.edu (S.L. Ferradal), inder_t@kids.wustl.edu (T.E. Inder).
[1]Co-first authors.

and society (Gilbert, 2006; Korvenranta et al., 2010). Furthermore, there is often a delay in the recognition of functional deficits due to few early behavioral manifestations and a paucity of effective early screening methods (Anderson et al., n.d.; Hack et al., 2005). While recent neuroimaging research using magnetic resonance imaging (MRI) and cranial ultrasonography has provided an understanding of the structural alterations associated with adverse neurodevelopmental outcomes in preterm infants (El-Dib et al., 2010), prediction of later disability remains modest. An enhanced understanding of the nature and timing of alterations in cerebral development associated with preterm birth (and improved predictive power for later disability) is likely to be achieved using methods based on cerebral function rather than structure (Seghier and Huppi, 2010).

Novel imaging methods using functional connectivity MRI (fcMRI) have been employed to define the brain's functional network architecture (Biswal et al., 1995; Fair et al., 2007; Fox et al., 2005; Fox and Raichle, 2007). These techniques are based on the synchronous, spontaneous fluctuations of cerebral blood flow in different regions of the brain that are functionally, yet not necessarily anatomically connected. These resting-state approaches have the advantage of mapping many different networks simultaneously and (importantly for infants) of not requiring the subject to perform tasks. Recent fcMRI studies have begun to establish the patterns of longitudinal functional network development (Fair et al., 2007; Fransson et al., 2007, 2009; Lin et al., 2008; Smyser et al., 2010). However, MRI techniques pose significant logistical barriers for use in preterm infants, largely related to challenges in transportation to the MRI scanner. Access is most difficult for the smallest and sickest prematurely born infants; yet these infants are at greatest risk for adverse neurodevelopmental outcomes. In addition, as cerebral structure and function are evolving rapidly from 24 weeks postmenstrual age (PMA) to term equivalence, frequent serial scanning (e.g., daily or weekly), which is not practical with MRI, may reveal the development of disease or disability over the neonatal intensive care course. Thus, the development of a bedside method to define functional networks in the preterm infant would allow serial evaluation of functional cerebral development in all infants within the neonatal intensive care unit setting.

Optical neuroimaging methods could potentially fulfill this role. Using a non-invasive measurement of hemoglobin absorption spectra as used in pulse oximetry, optical systems map the concentrations of both oxy- (HbO_2) and deoxy- (Hb_R) hemoglobin. At its simplest, this technique can be used with distinct (or "sparse") source-detector pairs, each over a brain region of interest—an implementation usually called near infrared spectroscopy (NIRS). However, standard NIRS systems take only a few widely distributed measurements and are thus limited with regard to comprehensive brain mapping. Additionally, they can suffer from drawbacks. First, as every measurement is a mixture of hemodynamics occurring in multiple tissue layers, it can be difficult to discriminate the brain signal of interest (Gregg et al., 2010). Second, the large gaps between measurements result in low spatial resolution and a decreased ability to correctly localize activations (White and Culver, 2010a).

In order to overcome these limitations, diffuse optical tomography (DOT) systems have been developed (Bluestone et al., 2001; Hebden et al., 2004; Joseph et al., 2006; Wylie et al., 2009; Zeff et al., 2007). Improved source and detection instrumentation allows measurements that overlap both laterally and in depth. The entire set of measurements can be inverted to create a 3D reconstruction of hemodynamic changes (in much the same way as a CT scan is derived from multiple X-rays) (Arridge, 1999). DOT systems thus have improved spatial resolution and the ability to distinguish superficial noise from the brain signal of interest.

As DOT combines the portability and cap-based scanning of EEG with spatial resolution high enough to create detailed cortical maps (White and Culver, 2010a, 2010b), it has the potential to be a powerful bedside clinical neuroimaging tool. Recently, functional connectivity methods have been extended to high density DOT (fcDOT) in adults (White et al., 2009) and have been subsequently developed with sparse NIRS topography in adults (Lu et al., 2010) and infants (Homae et al., 2010). In this paper, we apply fcDOT to bedside imaging of neonates within the first month of life, further developing pilot studies in infants that have demonstrated the feasibility of high-density imaging arrays in the neonatal environment (Liao et al., 2010). We show fcDOT images in both term and premature infants. Additionally, we show how these maps can be disrupted through brain injury. As these proof-of-concept results are extended, we expect that fcDOT can become an important diagnostic and prognostic tool for neonatologists.

Materials and methods

Subjects

Subjects were recruited from the nurseries of Barnes-Jewish and St. Louis Children's Hospitals. Informed consent was acquired from the infants' parents. The study was approved by the Human Research Protection Office of Washington University in St. Louis. We scanned three term-born and five premature infants. One preterm infant had a unilateral occipital stroke. Another preterm infant had significant morbidities including extreme prematurity (born at 23 5/7 weeks of gestation), chronic lung disease, high stage retinopathy of prematurity, and bowel perforation. This infant had evidence of evolving grade III intraventricular hemorrhage (IVH) on serial cranial ultrasounds, but the term-equivalent MRI of the head showed only minimal anatomical abnormalities. All other preterm infants had relatively less complicated hospital courses. The term-born infants were scanned within the first three days of life. Each premature infant was scanned once, at a time point based on availability during his/or hospitalized course (see Table 1 for specifics). Relevant demographic and clinical information about the patients is included in Table 1. All infants were scanned in their bassinets or incubators while quietly resting or sleeping (although sleep state was not actively monitored) (Liao et al., 2010).

DOT data collection

For this study, we used a custom-built high-density DOT system (Zeff et al., 2007) with an optode array consisting of 18 sources and 16 detectors (Fig. 1A) for 106 total measurements. Each source position consisted of two near infrared wavelengths (750 nm and 850 nm) of light emitting diodes (LEDs). The system operates in continuous-wave mode with a frame rate of 10.78 Hz. The imaging cap consisted of flexible optical fiber bundles embedded in a silicone array. This soft pad was held against the head using neoprene straps and Velcro. The array was placed just superior to the inion, in order to be superficial to the occipital (visual) cortex (Fig. 1B). All scans were taken within 2 h after feeding in an isolated, dimly lit room either in the nursery at Barnes-Jewish Hospital or in the Neonatal Intensive Care Unit (NICU) at St. Louis Children's Hospital. The total duration of the resting-state data acquisition ranged from 10 to 20 minutes depending on the cooperativeness of the infant.

Data pre-processing

Resting state data were acquired using the DOT system with good signal-to-noise well above the noise floor (Fig. 1C). The data were cleaned of both motion artifacts and superficial hemodynamic signals. Motion artifacts are visible as sharp changes in intensity across many channels in the raw intensity measurements. Using this visual identifier of motion, time periods with no visible artifacts were chosen for further analysis (yielding data of lengths between two and eleven minutes). The source-detector data was converted to log-

ratio data consistent with the tomographic data inversion routine (Rytov approximation) and was filtered to the frequency band of 0.009 to 0.08 Hz following fcMRI and fcDOT algorithms (Fox et al., 2005; White et al., 2009).

Physiological noise was reduced using a superficial signal regression procedure (Gregg et al., 2010). The source-detector measurements with the shortest separations (called first-nearest neighbors) are separated by 1 cm and are primarily sensitive to the scalp and skull. Second-nearest neighbors (2.2 cm separation) have significantly greater sensitivity to the brain. To remove systemic and superficial hemodynamics we linearly-regressed out an average of the first-nearest neighbor measurements from all of the individual measurements (Gregg et al., 2010; Saager and Berger, 2005, 2008; Zeff et al., 2007). In order to reject measurements with motion artifacts or poor optode coupling to the head, source-detector channels with high standard deviation (>7.5%) are excluded from further analysis. An average first-nearest neighbor measurement had a standard deviation of 1.6%, and an average second-nearest neighbor, 3.0%. So, the adopted standard deviation threshold can exclude abnormally large variations while preserving normal physiology. Within a range, the reconstruction is relatively insensitive to the exact threshold chosen. Across all sessions, this procedure kept 98% of first-nearest neighbor signals and 96% of second-nearest neighbor signals.

DOT head modeling and image reconstruction

Homogeneous head models with estimated optical properties have been widely used in previous evoked and resting-state studies (Hebden et al., 2002; Zeff et al., 2007) in both infants and adults. This approach is supported by studies showing that the use of differential measurements minimizes the errors introduced by either incorrect baseline optical properties (Strangman et al., 2003) or by a heterogeneous/homogeneous structural model mismatch (Gibson et al., 2005). While semi-infinite (Abdelnour et al., n.d.) or hemispherical models (Zeff et al., 2007) are common geometries for NIRS analysis, here we have developed a more realistic head model derived from a head atlas consisting of twelve T2-weighted MR images of healthy term-born infants. Using Mimics 3D modeling software, we segmented the outer surface of the MRI atlas and created a finite-element model consisting of 43,410 nodes and 260,246 tetrahedral elements (Fig. 1A). Homogeneous optical properties (absorption coefficient: μ_a and reduced scattering coefficient: μ'_s) were assumed for the whole head (μ_a=0.19 cm^{-1} μ'_s=12 cm^{-} at 750 nm and μ_a=0.19 cm^{-1} μ'_s=11 cm^{-1} at 850 nm, obtained from Strangman et al. (2003)). While these values were obtained from adults, studies comparing optical properties in adults and infants have generally shown similar optical properties in both groups (Fukui et al., 2003), and most NIRS/DOT studies of infants use adult values for relevant head-averaged optical constants (Gibson et al., 2003; Franceschini et al., 2007).The optode array was placed over the back of the head model just superior to the inion, as shown in Fig. 1A. Based on the anatomical model and the optode positions, a sensitivity matrix was generated using NIRFAST light modeling software (Dehghani et al., 2003). Volumetric reconstructions of absorption coefficient at both 750 nm and 850 nm co-registered with the anatomical MRI atlas were obtained. Three dimensional maps of concentration changes of HbO_2 and Hb_R were computed using the extinction coefficients of each hemoglobin species (Wray et al., 1988).

An average surface-based atlas of the neonatal cortex derived from the same cohort of term-born infants was used to perform 3D visualization of reconstructed DOT data. The surface was created following the method described in Hill et al. (2010), while the surface mapping was performed using Caret software (Van Essen et al., 2001).

Functional connectivity analysis

We analyzed resting-state brain functional connectivity in two manners. First, 6 mm spheres in the visual cortex were chosen as regions of interest (ROIs) based on anatomic landmarks (the inion and the calcarine sulcus). From these ROI positions, seed time traces were extracted for each of the three hemodynamic contrasts. These time courses were then correlated with every other voxel within the field of view to generate correlation (*r*) maps.

Second, we performed independent component analysis (ICA). After the imaging described above, we used FastICA (Hyvarinen, 1999) to perform temporal ICA on the sequence of images, with the same preprocessing steps and non-linearity function as were used in our previous study of adult visual activations (Markham et al., 2009). For each data set, we extracted between 10 and 20 independent components, from which components corresponding to the visual resting-state network were chosen. For the independent component (IC) selection, we followed an fcMRI approach in which templates are used to identify network patterns (Damoiseaux et al., 2006). Our IC selection is similar with the exception that a smaller number of independent components were estimated due to our smaller field of view. In particular, we used a bilateral template to identify the IC located over the visual cortex. If a bilateral pattern was not present, we identified the most defined unilateral response. In order to validate our selection, we analyzed the spectrum of the associated time course and verified that it exhibited high power within the functional connectivity frequency band (0.009 to 0.08 Hz). The excluded components exhibited patterns that can potentially be associated with artifacts such as head motion and physiological noise (Beckmann et al., 2005). This method to sorting ICs is similar to that used in fcMRI studies using ICA (Damoiseaux et al., 2006). The contribution of each IC to every voxel's time course is described by a weighting matrix that can be displayed as an image showing how the particular hemodynamic activity of that IC is spatially distributed through the brain. Whenever we display images of "independent components" we are actually displaying this weighting. As independent components are only unique up to a multiplicative constant, we normalize the maximum amplitude of each such image to one.

Low frequency power analysis

The measurement of resting-state networks (using either seed-based or ICA methods) could be a powerful method for determining whether functional connections are developing normally. However, they inherently discard the magnitude of the spontaneous fluctuations. To provide a more comprehensive assessment, we also spatially map the magnitude (power) of the variance in the low-frequency band. In principle, the strength of the variance in the hemodynamic signals is related to the local strength of intrinsic brain activity. Thus, we generated spatial maps of the measured variance of the hemoglobin time traces within each voxel over time (again, filtered to the 0.009 to 0.08 Hz frequency band associated with resting brain activity). Methods similar to this have recently been developed for examining brain aging with fMRI (Garrett et al., 2010).

Results

Data from the healthy term-born infants showed strong correlations between the two visual seeds in all three hemodynamic contrasts (Table 2). When the seed was placed in the left visual cortex, maps of correlation coefficients for each seed showed ipsilateral correlations as well as correlations with the contralateral visual hemisphere (Fig. 2A). Symmetric patterns were seen with the seed in the right visual hemisphere (Fig. 2B). Similar bilateral correlation patterns were seen in the visual cortices of premature infants with less complicated hospital courses (Figs. 2C-D). Correlation maps obtained for these six healthy subjects using right seeds in the visual cortex show a similar bilateral network (Fig. 3).

We also scanned two premature infants with complicated clinical courses. One had a large left hemisphere occipital stroke (Fig. 4A). In this infant (preterm5), seeds placed in either the right visual cortex or on the left side of the imaging domain (where an operator naïve of the stroke would expect the left visual cortex) generated only unilateral correlation patterns (Fig. 4B). In all three contrasts, the two seeds were uncorrelated (Table 2). This result shows that fcDOT can be sensitive to neuronal injury. We also performed fcDOT on a second prematurely born infant who had a complicated clinical course (preterm4), including prolonged mechanical ventilation, bowel perforations requiring multiple surgeries, and high grade retinopathy of prematurity requiring laser eye surgery. This infant had early evidence of grade III intraventricular hemorrhage (IVH) on serial cranial ultrasounds, but had minimal anatomical abnormalities noted on term-equivalent MRI (Fig. 5A). In this case, the analysis showed similar connectivity patterns in the visual network to those in healthy infants (Fig. 5B) and strong inter-hemispheric correlation coefficients (Table 2). A comparison of correlation values for all infant groups is shown in Fig. 6.

The seed-based method allows us to measure specific correlations, but can be sensitive to the exact placement of the seed location. To provide a complementary analysis without use of seeds, we also evaluated the visual resting-state network using ICA. Although quantitative comparisons between both methods are difficult due to differences in the data processing involved in each technique, the functional maps obtained using either ICA or correlation analysis show remarkably similar results. Bilateral components were found for both healthy term-born infants (Fig. 7A), preterm infants with relatively less complicated clinical course (Fig. 7B), and Preterm4 (the infant with the complicated clinical course without anatomical brain injury, Fig. 7C). ICA of the images from the preterm infant with the occipital stroke (Preterm5) showed only unilateral patterns. As expected, the right hemisphere correlation map resembles the ICA result (Fig. 7D). We also found a separate component that resembles the correlation map obtained with a seed placed over the left hemisphere. However, no ICs were found for Preterm5 that exhibited bilateral patterns as in the case of healthy infants.

Both ICA and seed-based methods are able to find correlated structures that in principle map functional connections. However, based on the data presented in this paper, we cannot make any claims about functional connectivity networks or correlations being different between premature and term infants. These results rather seem to show overall that (in the visual network at least) both groups of infants have similar correlation patterns and strength. While there are certainly small differences, we suspect that these are either due to physiological noise or instrument noise.

We also evaluated the utility of mapping the magnitude of the local variance in the low frequency band. Examination of the power spectrum of resting-state time traces of the left and right seeds showed that, in a healthy infant, the pattern of a 1/f curve (<0.1 Hz), and a pulse peak (2–3 Hz) is almost identical in both hemispheres (Fig. 8A). However, in the infant with the unilateral stroke, pulse was seen in both hemispheres, but the low frequency content was lower in the affected hemisphere (Fig. 8B).

Maps of the relative power in the frequency band corresponding to resting-state brain activity (0.009–0.08 Hz) showed highly bilateral patterns of resting-state brain activity in the healthy term-born infants (Fig. 9A) and as well as in preterm infants with less complicated clinical courses (Figs. 9B-C). However, in the infant with the stroke, we see an asymmetric pattern with attenuated power in the stroke area (Fig. 9D).

Discussion

In this paper, we have shown the results of functional connectivity analysis in the occipital cortex using both seed-based methods and ICA. Although quantitative comparisons between both methods are difficult due to differences in the data processing involved in each technique, the functional maps obtained using either ICA or correlation analysis show remarkably similar results. These analyses demonstrate strong bilateral functional connectivity within the visual network in both healthy preterm and term infants. While not all functional connectivity networks are fully-formed in preterm and term neonates, previous fMRI results have shown that bilateral occipital connections occur at all ages that we have measured here (Fransson et al., 2007; Smyser et al., 2010; Doria et al., 2010). Thus, this network is a good model system for the proof-of-principle of bedside mapping with optical neuroimaging. While our results exhibit small differences between individual neonates, further studies with larger populations are needed to allow full statistical analysis of any differences and to separate the contribution of various physiological noise sources. Such statistical methods, including Fischer *z*-transformations have been developed for fcMRI, and these techniques will need to be adapted for future fcDOT analysis.

The fcDOT results in the infant with the stroke demonstrate the feasibility of detecting ischemia. Correlation analysis shows only unilateral connectivity for the infant with an infarcted left occipital cortex. ICA supports this result, demonstrating only unilateral independent components. That we continue to see connectivity within the left hemisphere is likely due to correlated noise within the infarct. Each voxel is required to have a correlation value of 1 with itself. Due to DOT having a point-spread function about the same size as our seed-averaging ROI, any seed will be surrounded by an area of high correlation even if the signal is just noise. That the region of correlation extends beyond this point spread function is due to either contamination by superficial signals into deep signals or due to correlated motion of the infarcted tissue. In neither case would the correlation be due to neural signals since there are no functional neurons in the tissue volume. Furthermore, this result is not affected by the exact ROI chosen.

In total, we have shown how functional connectivity can be acquired at the bedside in the nursery and neonatal intensive care unit with diffuse optical tomography. The visual networks that we have found extend our preclinical work in healthy adults and represent the first diffuse optical tomography of resting-state networks in infants. Our results are in agreement with previous fcMRI literature of infants (Fransson et al., 2007, 2009; Lin et al., 2008; Smyser et al., 2010), where although there is controversy about unilateral sensorimotor networks, the visual network is always reported as bilateral. These results serve to validate neonatal fcDOT in a well-studied network against the gold standard of fcMRI.

In contrast, in an fcNIRS study of infants (Homae et al., 2010), the authors only found a bilateral visual network develop at 3 months of age. It might be that their study did not see a visual network due to contamination from superficial artifacts, which are of major concern in NIRS studies and can lead to spurious reporting of hemodynamic signals. The methodology used in this paper, including superficial signal regression and tomographic image reconstructions, has been shown to have better brain specificity than NIRS (Gregg et al., 2010; Liao et al., 2010; Saager and Berger, 2008; Boden et al., 2007). Within the context of functional connectivity, in our earlier study of adults, we did see that, when linear noise regression methods were not used, networks could be hidden by artifacts from both superficial/systemic contaminants and noise from optode motion (White et al., 2009).

Although the visual cortex was a good starting point, it is not a cortical area that is especially vulnerable to injury in premature infants. Despite these limitations, the results shown here do demonstrate the promise for the clinical utility of fcDOT. The bilateral correlation pattern seen in healthy infants is disrupted specifically within a subject with occipital cortex injury. Future work is needed to extend fcDOT imaging to brain regions that are more clinically relevant, especially the motor network (of relevance to cerebral palsy) and the default mode network (which has seen growing interest in cognitive neuroscience). As DOT is limited in its depth of penetration, it will thus most likely be unable to map the entirety of these networks (for example, it might not be able to detect the cingulate portions of the default network). However, while not a full mapping, even a limited evaluation of these connections would hopefully yield information about the state of various brain networks, white matter integrity, and ischemia. Bedside measurements, even with limited field-of-view, could serve as a screening test to select at-risk infants for a more complete anatomic and functional MRI evaluation.

While, in the case of the occipital stroke, the stroke is immediately obvious from a structural MRI, relying on structural MRI for diagnosis is not an ideal clinical scenario. First, it is extremely difficult to predict when a future injury will occur. Thus, a method which can offer imaging at multiple time points at the bedside holds more promise for detecting potential indicators of developing injury. With longitudinal imaging, pre-injury conditions might be able to be detected before they have progressed to such an irreversible stage, thus allowing early intervention. Additionally, functional connectivity measurements might be able to detect more subtle injury, such as lower correlations due to white matter injury that could progress to cognitive deficits, but are not noticeable on anatomic imaging until far advanced.

In addition to functional connectivity, we also studied the possible role of low frequency power maps. We hypothesized that such a measure provides an alternate metric of each cortical area's function and might detect regions of injury independent of seed placement. As there are non-neuronal physiological processes that also have 1/f spectra, we would not expect low frequency power to be completely abolished in the affected area. With this metric, we also saw bilateral patterns in healthy infants. In the infant with the occipital stroke, low frequency power was stronger in the healthy hemisphere. Differences in the low frequency power spectrum between subjects can also be noticed. It may be that these differences relate to changes in neurovascular coupling, cerebral blood flow (CBF), or cerebral blood volume (CBV) during development. A quantitative analysis of power spectrum differences will require studies with greater numbers of subjects. We expect that the power mapping technique could be a helpful clinical tool along-side more common functional connectivity measures. Low frequency power could be measured continuously in all cortical locations without need for user input. More detailed measures of functional connectivity, checking for the integrity of networks, could be performed at various longitudinal time points or when deficits in intrinsic brain activity are suspected from the power maps.

The brain's resting state can be studied both through the connections between regions and through metabolism. While, we have studied purely the former in this paper, recent research (Vaishnavi et al., 2010) has shown that brain networks can be intimately linked to metabolic variations. Optical imaging has a long history of studying CBV, tissue oxygenation (S_tO_2), CBF, and the cerebral rate of oxygen metabolism ($CMRO_2$) (Bouchard et al., 2009; Culver et al., 2003, 2009; Devor et al., 2003; Dunn et al., 2005; Siegel et al., 2003; Villringer and Chance, 1997). Recent studies in neonates have shown that baseline hemodynamics evolve throughout early development (Roche-Labarbe et al., 2010). One of the advantages of functional correlation analysis is that it inherently normalizes out absolute differences in

parameters such as signal intensity. Thus, global differences in CBV and the strength of neurovascular coupling should not affect the results presented in this paper, especially as we examine only one region of cortex. However, as multiple regions of the brain might develop at different rates, this effect might become more important in future investigations.

In the current study, we restricted the measurements to a small cortical area (visual cortex) in order to provide higher imaging quality. However, with this limited brain coverage, we cannot explore interesting issues such as negative correlations, as in several fMRI studies (Fox et al., 2009). While some works argue that anticorrelations are caused by the global signal regression method involved in the standard fMRI analysis (Birn et al., 2006; Weissenbacher et al., 2009), others believe that these anti-correlated networks have an underlying physiological meaning (Fox et al., 2005; Fox and Raichle, 2007). By expanding the field of view, we would expect to be able to begin interpreting these negative correlations in the fcDOT maps.

Future DOT systems will involve greater numbers of optodes, and thus be able to combine high quality imaging with larger fields of view which, in turn, will allow the study of more functional networks and their interactions. Although new developments can potentially provide whole-head coverage, certain challenges such as ergonomics and inversion problems will need to be considered. Regarding ergonomics, one must build a cap to fit a certain number of fibers optics on the head. Multiple labs are working on developing improvements to make whole-head, high-density imaging and we suspect that it will occur in the near future. A second difficulty will then be computing power. The inversion problem is already computationally intense even with the limited number of measurements and voxels currently involved in regional imaging. Multi-scale techniques or other methods of reducing the matrix size in the inversion step will probably need to be adapted for use in whole-brain functional imaging.

The choice of the appropriate head model to use for any optical neuroimaging study is a tradeoff between algorithmic simplicity and reconstruction accuracy. The ideal geometry would be an anatomic model of the scalp, skull, CSF, and brain with individual optical properties for each region. The majority of NIRS and DOT studies have instead used simplified geometries (semi-infinite or hemispherical) with homogeneous or two-layered optical properties. These methods have worked well in adult populations. However, as we expected neonatal heads to depart more from these geometries, we used an MRI-derived atlas of the neonatal head surface. While segmentation algorithms have been developed for adult anatomic MRIs to assign optical properties to individual voxels, such methods have not yet been derived for infants, due to relatively lower resolution and differences in T1- and T2-contrast sensitivity of the brain. Thus, we used a homogenous model. The utility of homogeneous optical properties is supported by several studies showing that ratiometric data (signal variance divided by the average baseline value) mitigates potential model mismatch (Gibson et al., 2005; Strangman et al., 2003). Further, the correlation method used in functional connectivity divides out the magnitude of the variance in the data. Thus, the current results are less sensitive to errors in the magnitude of the response. Nonetheless, tissue-specific head modeling is becoming more accessible and future work will likely provide improved imaging performance (Custo et al., 2010; Heiskala et al., 2009).

A potential challenge in imaging infants is the variable sleep states encountered. On the one hand, recent work with fMRI has shown that within three primary sensory networks (visual, auditory, and somatomotor) and three association networks (attention, default, executive), functional connectivity is maintained throughout wakefulness to light sleep (Larson-Prior et al., 2009). On the other hand, during deep sleep, some reduction in connections within the default network has been observed (Horovitz et al., 2008). Studies in infants have shown no

differences between functional connectivity in deep sleep and sedation (Doria et al., 2010). Sleep state variances in our study are most likely between stages of light sleep and are unlikely to influence the visual network results of this paper. However, future fcDOT studies would benefit from monitoring the sleep state by EEG in order to account for a potential source of variability between and within groups.

In conclusion, we have shown that bedside imaging of functional connectivity of both term and preterm neonates is possible within the clinical environment. This methodology may provide important diagnostic and prognostic information, allowing clinicians to identify "functional lesions" and track functional development at the bedside. In addition, fcDOT can be a useful tool to study the effects of various clinical interventions (such as ventilation strategies, nutrition, and pharmacological therapies) and clinical risk factors (e.g., infections and other co-morbidities) on the development of neural function during the initial hospitalization. Functional along with anatomical lesions can further be used to better predict future neurodevelopmental outcomes. Additionally, it might be possible to identify optical imaging markers to define pre-injury conditions and allow early intervention before damage has become more extensive. In these ways, fcDOT can complement the research potential of fcMRI by adding longitudinal bedside imaging.

Acknowledgments

We thank Martin Olevitch for help with DOT software, Jim Alexopoulos and Donna Dierker for help with Caret software, and Amanda Jezusko for assisting with recruiting and clinical scanning.

Funding

This work was supported in part by NIH grants R01-EB009233 (J.P.C), R21-EB007924 (J.P.C.), T90-DA022871 (Imaging Science Fellowship, B.R.W.), the Medical Scientist Training Program (B.R.W.) UL1RR024992 (post-doctoral research training grant, S.M.L.), Fulbright Science and Technology Ph.D. Award (S.L.F.). J.P.C and Washington University have financial interests in Cephalogics LLC based on a license of related optical imaging technology by the university to Cephalogics LLC.

Abbreviations

Fc	functional connectivity
DOT	diffuse optical tomography
HbO_2	oxyhemoglobin
HbR	deoxyhemoglobin
HbT	total hemoglobin

References

Abdelnour F, Genovese C, Huppert T. Hierarchical Bayesian regularization of reconstructions for diffuse optical tomography using multiple priors. Biomed. Opt. Express. 2010; 1(4):1084–1103. [PubMed: 21258532]

Anderson PJ, et al. Underestimation of developmental delay by the new Bayley-III Scale. Arch. Pediatr. Adolesc. Med. 2010; 164(4):352–356. [PubMed: 20368488]

Arridge SR. Optical tomography in medical imaging. Inverse Prob. 1999; 15(2):R41–R93.

Beckmann CF, et al. Investigations into resting-state connectivity using independent component analysis. Phil. Trans. R. Soc. Lond. B Biol. Sci. 2005; 360(1457):1001–1013. [PubMed: 16087444]

Birn RM, et al. Separating respiratory-variation-related fluctuations from neuronal-activity-related fluctuations in fMRI. Neuroimage. 2006; 31(4):1536–1548. [PubMed: 16632379]

Biswal B, et al. Functional connectivity in the motor cortex of resting human brain using echo-planar MRI. Magn. Reson. Med. 1995; 34(4):537–541. [PubMed: 8524021]

Bluestone AY, et al. Three-dimensional optical tomography of hemodynamics in the human head. Opt. Express. 2001; 9(6):272–286. [PubMed: 19421298]

Boden S, et al. The oxygenation response to functional stimulation: is there a physiological meaning to the lag between parameters? Neuroimage. 2007; 36(1):100–107. [PubMed: 17400478]

Bouchard MB, et al. Ultra-fast multispectral optical imaging of cortical oxygenation, blood flow, and intracellular calcium dynamics. Opt. Express. 2009; 17(18):15670–15678. [PubMed: 19724566]

Culver JP, et al. Diffuse optical tomography of cerebral blood flow, oxygenation, and metabolism in rat during focal ischemia. J. Cereb. Blood Flow Metab. 2003; 23(8):911–924. [PubMed: 12902835]

Culver JP, et al. Topics in biomedical optics: introduction to the feature issue. Appl. Opt. 2009; 48(10):TBO1–TBO2. [PubMed: 19340130]

Custo A, et al. Anatomical atlas-guided diffuse optical tomography of brain activation. Neuroimage. 2010; 49(1):561–567. [PubMed: 19643185]

Damoiseaux JS, et al. Consistent resting-state networks across healthy subjects. Proc. Natl. Acad. Sci. U. S. A. 2006; 103(37):13848–13853. [PubMed: 16945915]

Dehghani H, et al. Three-dimensional optical tomography: resolution in small-object imaging. Appl. Opt. 2003; 42(16):3117–3128. [PubMed: 12790463]

Devor A, et al. Coupling of total hemoglobin concentration, oxygenation, and neural activity in rat somatosensory cortex. Neuron. 2003; 39(2):353–359. [PubMed: 12873390]

Doria V, et al. Emergence of resting state networks in the preterm human brain. Proc. Natl. Acad. Sci. U. S. A. 2010; 107(46):20015–20020. [PubMed: 21041625]

Dunn AK, et al. Spatial extent of oxygen metabolism and hemodynamic changes during functional activation of the rat somatosensory cortex. Neuroimage. 2005; 27(2):279–290. [PubMed: 15925522]

El-Dib M, et al. Neuroimaging and neurodevelopmental outcome of premature infants. Am. J. Perinatol. 2010; 27(10):803–818. [PubMed: 20486038]

Fair DA, et al. Development of distinct control networks through segregation and integration. Proc. Natl. Acad. Sci. U. S. A. 2007; 104(33):13507–13512. [PubMed: 17679691]

Fanaroff AA, Hack M, Walsh MC. The NICHD neonatal research network: changes in practice and outcomes during the first 15 years. Semin. Perinatol. 2003; 27(4):281–287. [PubMed: 14510318]

Fox MD, Raichle ME. Spontaneous fluctuations in brain activity observed with functional magnetic resonance imaging. Nat. Rev. Neurosci. 2007; 8(9):700–711. [PubMed: 17704812]

Fox MD, et al. The human brain is intrinsically organized into dynamic, anticorrelated functional networks. Proc. Natl. Acad. Sci. U. S. A. 2005; 102(27):9673–9678. [PubMed: 15976020]

Fox MD, et al. The global signal and observed anticorrelated resting state brain networks. J. Neurophysiol. 2009; 101(6):3270–3283. [PubMed: 19339462]

Franceschini MA, et al. Assessment of infant brain development with frequency-domain near-infrared spectroscopy. Pediatr. Res. 2007; 61(5 Pt 1):546–551. [PubMed: 17413855]

Fransson P, et al. Resting-state networks in the infant brain. Proc. Natl. Acad. Sci. U. S. A. 2007; 104(39):15531–15536. [PubMed: 17878310]

Fransson P, et al. Spontaneous brain activity in the newborn brain during natural sleep—an fMRI study in infants born at full term. Pediatr. Res. 2009; 66(3):301–305. [PubMed: 19531974]

Fukui Y, Ajichi Y, Okada E. Monte Carlo prediction of near-infrared light propagation in realistic adult and neonatal head models. Appl. Opt. 2003; 42(16):2881–2887. [PubMed: 12790436]

Garrett DD, et al. Blood oxygen level-dependent signal variability is more than just noise. J. Neurosci. 2010; 30(14):4914–4921. [PubMed: 20371811]

Gibson A, et al. Optical tomography of a realistic neonatal head phantom. Appl. Opt. 2003; 42(16): 3109–3116. [PubMed: 12790462]

Gibson AP, et al. Linear and nonlinear reconstruction for optical tomography of phantoms with nonscattering regions. Appl. Opt. 2005; 44(19):3925–3936. [PubMed: 16004037]

Gilbert WM. The cost of preterm birth: the low cost versus high value of tocolysis. Brit. J. Obstet. Gynaec. 2006; 113(Suppl 3):4–9.

Gregg NM, et al. Brain specificity of diffuse optical imaging: improvements from superficial signal regression and tomography. Front. Neuroenergetics. 2010; 2(14):1–8. [PubMed: 20162100]

Hack M, et al. Poor predictive validity of the Bayley Scales of Infant Development for cognitive function of extremely low birth weight children at school age. Pediatrics. 2005; 116(2):333–341. [PubMed: 16061586]

Hebden JC, et al. Three-dimensional optical tomography of the premature infant brain. Phys. Med. Biol. 2002; 47(23):4155–4166. [PubMed: 12502040]

Hebden JC, et al. Imaging changes in blood volume and oxygenation in the newborn infant brain using three-dimensional optical tomography. Phys. Med. Biol. 2004; 49(7):1117–1130. [PubMed: 15128193]

Heiskala J, et al. Probabilistic atlas can improve reconstruction from optical imaging of the neonatal brain. Opt. Express. 2009; 17(17):14977–14992. [PubMed: 19687976]

Hill J, et al. A surface-based analysis of hemispheric asymmetries and folding of cerebral cortex in term-born human infants. J. Neurosci. 2010; 30(6):2268–2276. [PubMed: 20147553]

Holsti L, Grunau RV, Whitfield MF. Developmental coordination disorder in extremely low birth weight children at nine years. J. Dev. Behav. Pediatr. 2002; 23(1):9–15. [PubMed: 11889346]

Homae F, et al. Development of global cortical networks in early infancy. J. Neurosci. 2010; 30(14): 4877–4882. [PubMed: 20371807]

Horovitz SG, et al. Low frequency BOLD fluctuations during resting wakefulness and light sleep: a simultaneous EEG-fMRI study. Hum. Brain Mapp. 2008; 29(6):671–682. [PubMed: 17598166]

Hyvarinen A. Fast and robust fixed-point algorithms for independent component analysis. IEEE Trans. Neural Netw. 1999; 10(3):626–634. [PubMed: 18252563]

Joseph DK, et al. Diffuse optical tomography system to image brain activation with improved spatial resolution and validation with functional magnetic resonance imaging. Appl. Opt. 2006; 45(31): 8142–8151. [PubMed: 17068557]

Korvenranta E, et al. Impact of very preterm birth on health care costs at five years of age. Pediatrics. 2010; 125(5):e1109–e1114. [PubMed: 20368320]

Larson-Prior LJ, et al. Cortical network functional connectivity in the descent to sleep. Proc. Natl. Acad. Sci. U. S. A. 2009; 106(11):4489–4494. [PubMed: 19255447]

Liao SM, et al. Neonatal hemodynamic response to visual cortex activity: a high-density NIRS study. J. Biomed. Opt. 2010; 15(2):026010. [PubMed: 20459255]

Lin W, et al. Functional connectivity MR imaging reveals cortical functional connectivity in the developing brain. Am J Neuroradiol. 2008; 29:1883–1889. [PubMed: 18784212]

Lu CM, et al. Use of fNIRS to assess resting state functional connectivity. J. Neurosci. Meth. 2010; 186(2):242–249.

Markham J, et al. Blind identification of evoked human brain activity with independent component analysis of optical data. Hum. Brain Mapp. 2009; 30(8):2382–2392. [PubMed: 19180556]

Roche-Labarbe N, et al. Noninvasive optical measures of CBV, StO_2, CBF index, and $rCMRO_2$ in human premature neonates' brains in the first six weeks of life. Hum. Brain Mapp. 2010; 31(3): 341–352. [PubMed: 19650140]

Saager RB, Berger AJ. Direct characterization and removal of interfering absorption trends in two-layer turbid media. J. Opt. Soc. Am. A Opt. Image Sci. Vis. 2005; 22(9):1874–1882. [PubMed: 16211814]

Saager R, Berger A. Measurement of layer-like hemodynamic trends in scalp and cortex: implications for physiological baseline suppression in functional near-infrared spectroscopy. J. Biomed. Opt. 2008; 13(3):034017. [PubMed: 18601562]

Seghier ML, Huppi PS. The role of functional magnetic resonance imaging in the study of brain development, injury, and recovery in the newborn. Semin. Perinatol. 2010; 34(1):79–86. [PubMed: 20109975]

Siegel AM, et al. Temporal comparison of functional brain imaging with diffuse optical tomography and fMRI during rat forepaw stimulation. Phys. Med. Biol. 2003; 48(10):1391–1403. [PubMed: 12812454]

Smyser CD, et al. Longitudinal analysis of enural network development in preterm infants. Cereb. Cortex. 2010; 20(12):2852–2862. [PubMed: 20237243]

Strangman G, Franceschini MA, Boas DA. Factors affecting the accuracy of near-infrared spectroscopy concentration calculations for focal changes in oxygenation parameters. Neuroimage. 2003; 18(4):865–879. [PubMed: 12725763]

Taylor HG, et al. Longitudinal outcomes of very low birth weight: neuropsychological findings. J. Int. Neuropsychol. Soc. 2004; 10(2):149–163. [PubMed: 15012835]

Vaishnavi SN, et al. Regional aerobic glycolysis in the human brain. Proc. Natl. Acad. Sci. U. S. A. 2010; 107(41):17757–17762. [PubMed: 20837536]

Van Essen DC, et al. An integrated software suite for surface-based analyses of cerebral cortex. J. Am. Med. Inform. Assoc. 2001; 8(5):443–459. [PubMed: 11522765]

Villringer A, Chance B. Non-invasive optical spectroscopy and imaging of human brain function. Trends Neurosci. 1997; 20(10):435–442. [PubMed: 9347608]

Weissenbacher A, et al. Correlations and anticorrelations in resting-state functional connectivity MRI: a quantitative comparison of preprocessing strategies. Neuroimage. 2009; 47(4):1408–1416. [PubMed: 19442749]

White BR, Culver JP. A quantitative evaluation of high-density diffuse optical tomography: in vivo resolution and mapping performance. J. Biomed. Opt. 2010a; 15(2):026006. [PubMed: 20459251]

White BR, Culver JP. Phase-encoded retinotopy as an evaluation of diffuse optical neuroimaging. Neuroimage. 2010b; 49(1):568–577. [PubMed: 19631755]

White BR, et al. Resting-state functional connectivity in the human brain revealed with diffuse optical tomography. Neuroimage. 2009; 47(1):148–156. [PubMed: 19344773]

Woodward LJ, et al. Very preterm children show impairments across multiple neurodevelopmental domains by age 4 years. Arch. Dis. Child. Fetal Neonatal Ed. 2009; 94(5):F339–F344. [PubMed: 19307223]

Wray S, et al. Characterization of the near infrared absorption spectra of cytochrome aa3 and haemoglobin for the non-invasive monitoring of cerebral oxygenation. Biochim. Biophys. Acta. 1988; 933(1):184–192. [PubMed: 2831976]

Wylie GR, et al. Using co-variations in the Hb signal to detect visual activation: a near infrared spectroscopic imaging study. Neuroimage. 2009; 47(2):473–481. [PubMed: 19398013]

Zeff BW, et al. Retinotopic mapping of adult human visual cortex with high-density diffuse optical tomography. Proc. Natl. Acad. Sci. U. S. A. 2007; 104(29):12169–12174. [PubMed: 17616584]

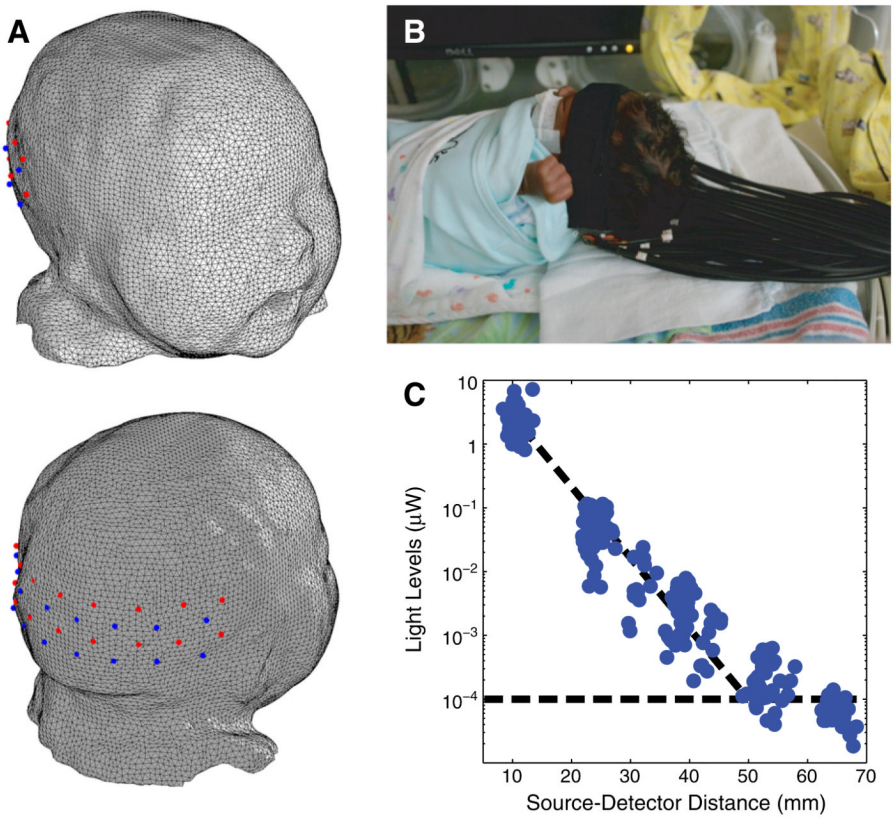

Fig. 1.

Bedside functional imaging of infants with DOT. (A) Infant head model and visual cortex imaging pad with 18 sources (red) and 16 detectors (blue), placed over the occipital cortex. (B) Photograph of the optical probe on a premature infant in an isolette. (C) Detected light level vs. source-detector separation on an infant. All first- and second-nearest neighbor pairs were detected simultaneously and were well above the noise floor (shown by the horizontal dotted line).

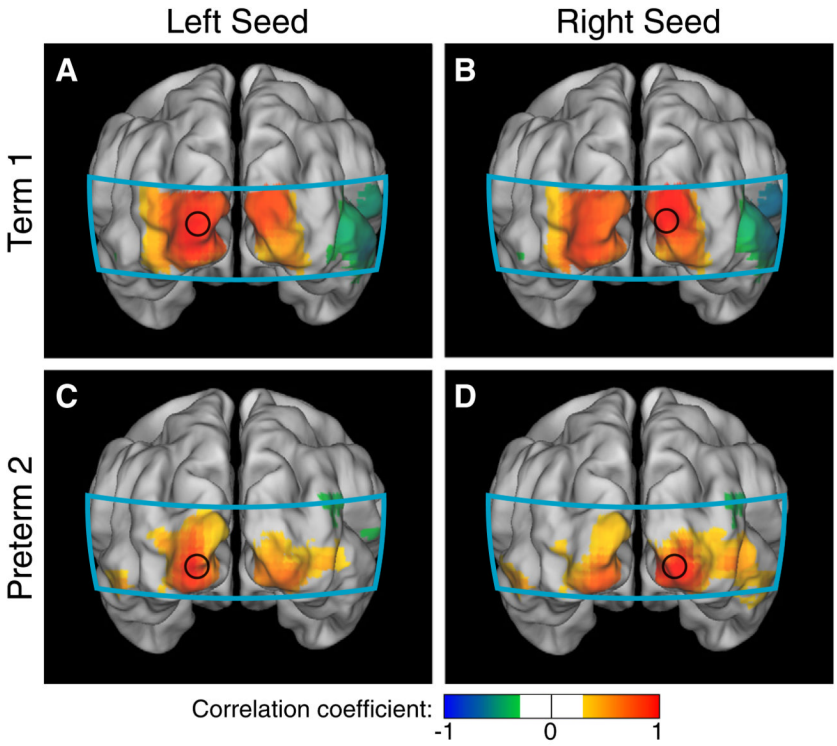

Fig. 2.

Neonatal fcDOT using seed-based correlation analysis in the visual cortex (HbO_2). (A, B) Correlation maps using seeds placed in the left and right visual cortices of a healthy term infant. Note the strong ipsilateral and contralateral correlations. (C,D) Correlation maps in a preterm infant with relatively less complicated clinical course, which also show bilateral correlation patterns. (All correlation images are scaled from r=−1 to 1 and have a threshold at $|r|$>0.3. The area covered by the imaging pad is shown in cyan.).

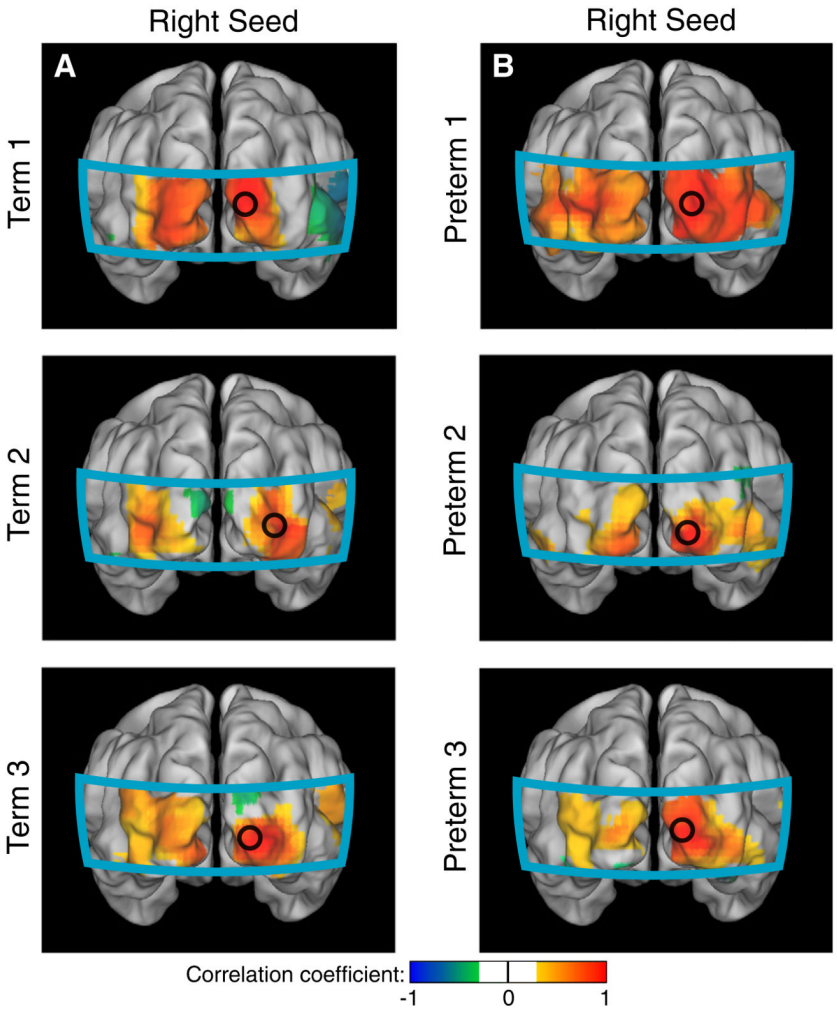

Fig. 3.

Correlation maps obtained for six infants without significant morbidities using right seeds in the visual cortex (HbO_2). (A) Individual correlation maps of three healthy term-born infants. (B) Similar correlation patterns were obtained for three preterm infants with relatively less complicated clinical courses.

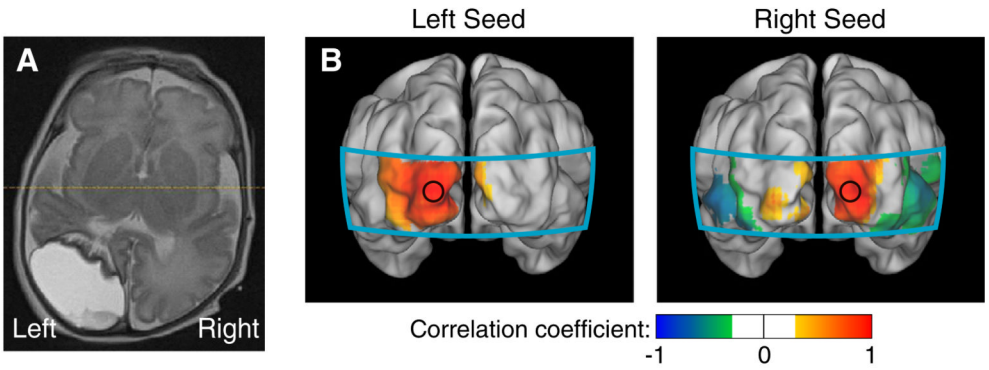

Fig. 4.

Neonatal fcDOT in a preterm infant with an occipital stroke (HbO_2). (A) An axial slice (neurological orientation) of a T2-weighted MRI of this infant done at approximately 36 weeks corrected gestational age, showing the stroke. (B) Correlation maps using seeds placed where the left and right visual cortices are expected to be. In both cases, we see only unilateral correlations. (All correlation images are scaled from r=−1 to 1.).

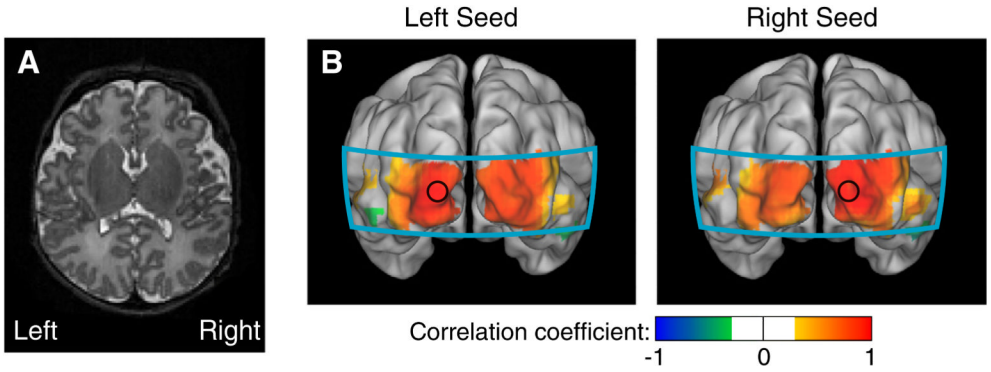

Fig. 5.

Neonatal fcDOT in a preterm infant with a complicated clinical course. (HbO_2). (A) An axial slice (neurological orientation) of a T2-weighted MRI showing minimal anatomical abnormalities at term-equivalent age, just prior to discharge. However, there appears to be white matter changes in the periventricular regions. (B) Correlation maps using seeds placed in the left and right visual cortices. We see the bilateral correlation patterns of a healthy visual cortex (all correlation images are scaled from r=−1 to 1).

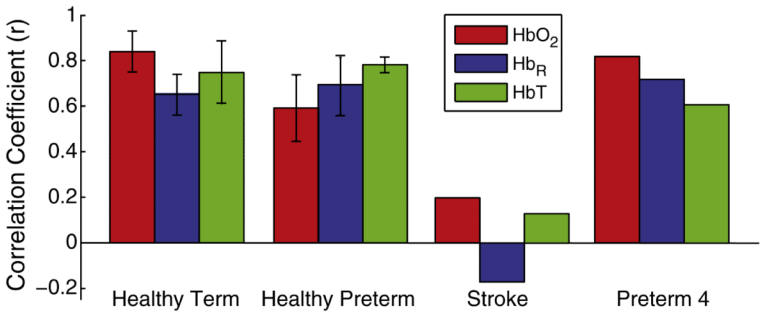

Fig. 6.

Average interhemispheric correlation coefficients for all infant groups and all three hemodynamic contrasts. Error bars show standard deviation over subjects (except for groups with only one subject).

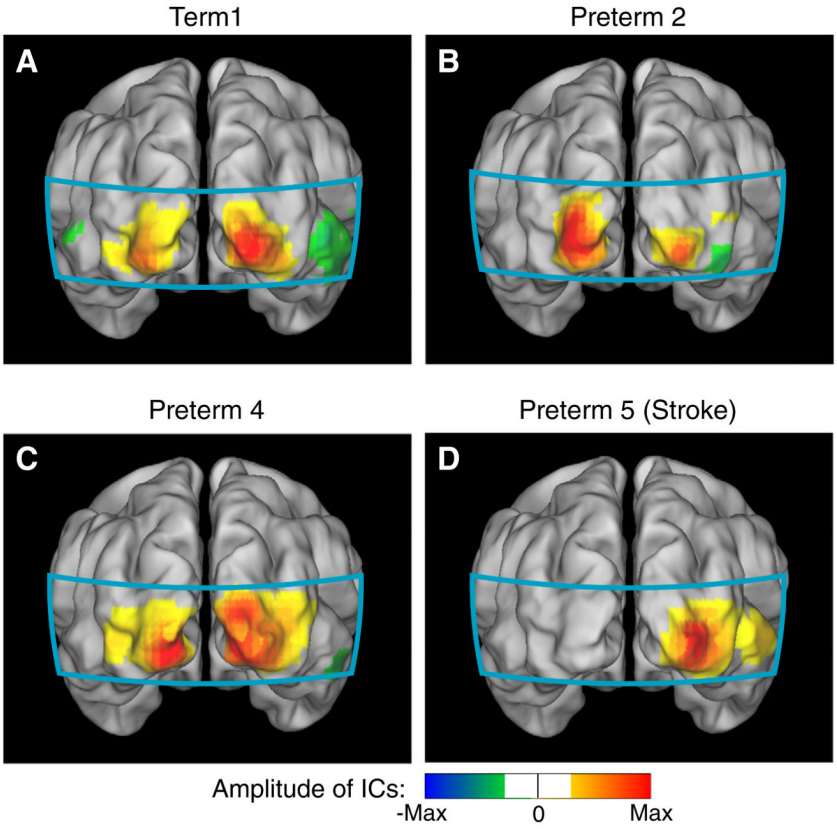

Fig. 7.

Neonatal fcDOT using independent component analysis (HbO_2). (A) Independent component (IC) in a healthy term infant showing a bilateral pattern (similar to Figs. 2A-B). (B) IC for a preterm infant with no significant anatomical brain injury (compare to Figs. 2C-D). (C) IC for the preterm infant with a complicated clinical course (compare to Fig. 5B). (D) Unilateral IC in the infant with the unilateral occipital stroke (compare to Fig. 4B). All components are scaled to their maximum, keeping zero at the center of the color scale, and the sign convention is that the strong "correlations" are positive; since ICA is unique only up to a multiplicative constant. The color scale threshold is similar to seed-based analysis.

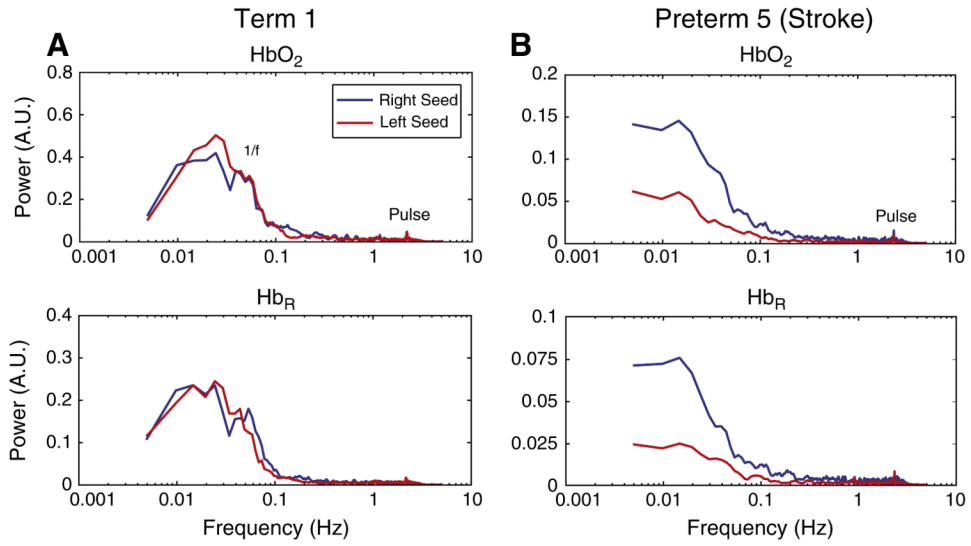

Fig. 8.

Resting-state DOT power spectra in neonates (HbO_2 and Hb_R). (A) In the healthy term-born infant we can see a 1/f curve as well as pulse peaks in both visual hemispheres. (B) In the infant with a left occipital stroke, we can still see systemic physiology in the affected hemisphere (pulse, and some 1/f fluctuations), but low frequency power is markedly lower, an indication of the lack of brain activity.

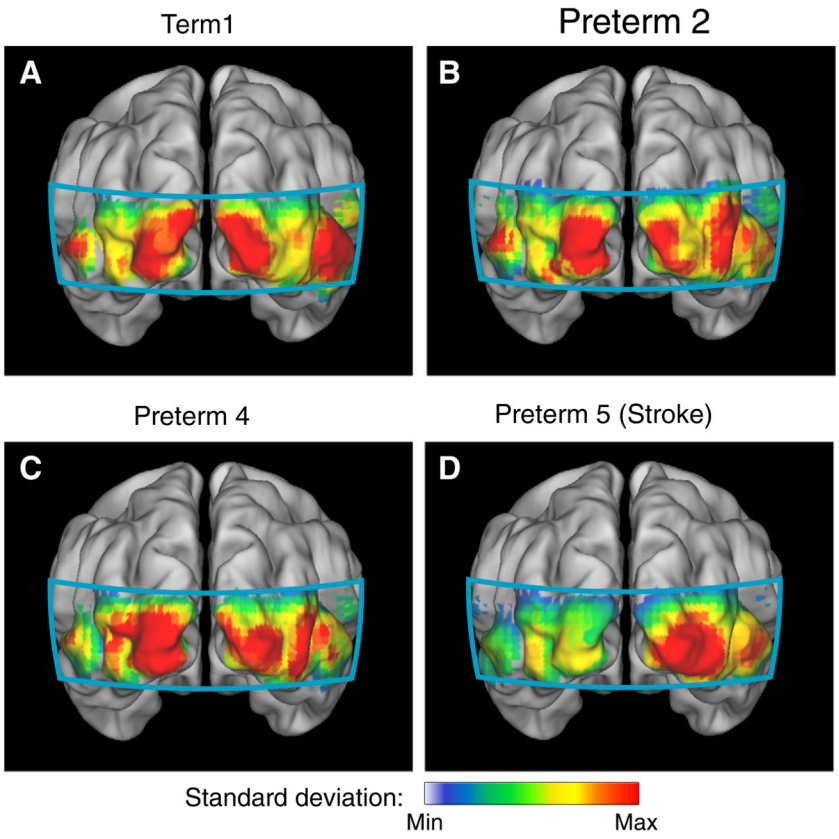

Fig. 9.

Maps of resting-state low frequency power (Hb_R). (A) Maps of low frequency power in a healthy term neonate. Note the bilateral pattern. (B, C) A similar bilateral power is seen in preterm infants with no significant anatomical injuries. (D) In the low frequency power map, power is only seen in the intact hemisphere in the infant with occipital stroke.

Table 1

Subject demographic and clinical information.

Subject code	Gestational age at delivery	Gestational age at DOT scan	Relevant clinical remarks
Term1	38 6/7	39 1/7	Healthy term infant
Term2	41 1/7	41 3/7	Healthy term infant
Term3	39 0/7	39 2/7	Healthy term infant
Preterm1	30 6/7	33 3/7	IUGR *, no known CNS injury
Preterm2	28 2/7	30 1/7	IUGR *, BPD †, grade I IVH **
Preterm3	24 6/7	32 5/7	BPD †, no known CNS injury
Preterm4	23 5/7	39 2/7	BPD †, intestinal perforation, ROP ‡, grade III IVH **
Preterm5	30	40	BPD † left occipital hemorrhage

* IUGR = intrauterine growth retardation

† BPD = bronchopulmonary dysplasia

** IVH = intraventricular hemorrhage

‡ ROP = retinopathy of prematurity.

Table 2

Interhemispheric visual correlation values (Pearson's correlations) in 8 infants.

Subject code	HbO_2	Hb_R	Hb_T
Term1	0.84	0.93	0.75
Term2	0.68	0.56	0.73
Term3	0.65	0.90	0.68
Preterm1	0.76	0.77	0.55
Preterm2	0.57	0.46	0.74
Preterm3	0.80	0.79	0.74
Preterm4	0.82	0.72	0.61
Preterm5	0.19	−0.17	0.13

HbO_2 = oxy, Hb_R = deoxy, Hb_T = total.